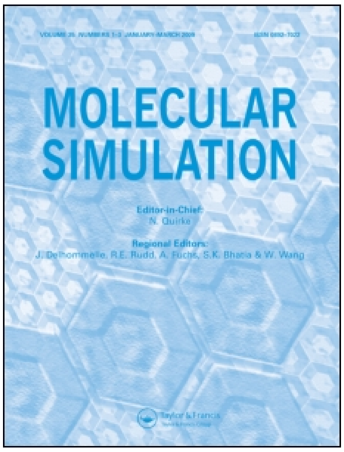

Molecular Simulation
Publication details, including instructions for authors and subscription information:
http://www.informaworld.com/smpp/title~content=t713644482

An *in-silico* study of solvent effects on the Kolbe-Schmitt reaction using a DFT method

I. Stanescu[a]; R. R. Gupta[a]; L. E. K. Achenie[a]
[a] Department of Chemical Engineering, University of Connecticut, Storrs, CT, USA

To cite this Article Stanescu, I. , Gupta, R. R. and Achenie, L. E. K.(2006) 'An *in-silico* study of solvent effects on the Kolbe-Schmitt reaction using a DFT method', Molecular Simulation, 32: 3, 279 — 290
To link to this Article: DOI: 10.1080/08927020600615000
URL: http://dx.doi.org/10.1080/08927020600615000

Molecular Simulation, Vol. 32, Nos. 3–4, 15 March–April 2006, 279–290

An *in-silico* study of solvent effects on the Kolbe–Schmitt reaction using a DFT method

I. STANESCU, R. R. GUPTA and L. E. K. ACHENIE*

Department of Chemical Engineering, University of Connecticut, 191 Auditorium Road, Storrs, CT 06269, USA

(Received December 2005; in final form January 2006)

It has been known empirically that some solvents facilitate homogeneity in the reaction mixture and potentially improve the reaction rate of the Kolbe–Schmitt reaction. The focus of this study is to reconcile the empirical observation with an *in-silico* study of the Kolbe–Schmitt reaction mechanism using density functional methods (B3LYP) and to investigate solvent effects on this reaction. The candidate solvents were designed using group-contribution based computer aided molecular design (CAMD) and tested using density functional methods for solvation calculations.

Keywords: Kolbe–Schmitt reaction; Density functional theory; Computer aided molecular design; Solvent design

1. Introduction

Aromatic hydroxy carboxylic acids are important intermediates in the synthesis of numerous products, including pharmaceuticals such as Aspirin™, antiseptic agents, fungicidal agents, dyes, polyesters, high-polymeric liquid crystals, color-developing agents and textile assistants. The conventional method for preparing these acids is the Kolbe–Schmitt reaction [1–4]. Usually, this reaction is carried out by introducing dry carbon dioxide under pressure over dry alkali metal aryloxides or by rapidly passing carbon dioxide through the melted alkali metal aryloxide. The Kolbe–Schmitt reaction has also been reported to take place in solution or suspension, allowing intensified stirring of the reaction mixture. The conditions of the Kolbe–Schmitt reaction vary over a wide range, depending on the starting alkali metal aryloxide, the procedure used for carrying out the reaction, the use of solvents or suspension media, the degree of dryness (presence of water) and a few other factors [5].

Kolbe [6] first formulated salicylic acid by heating sodium phenoxide with carbon dioxide at atmospheric pressure and acidifying the resulting sodium salicylate solution (figure 1).

Kolbe obtained yields below 50%. In the course of the reaction, despite absolutely dry conditions, half of the initial amount of phenol distilled from the reaction mixture, usually at low CO_2 pressure and high temperature, when the following side reactions (figure 2) occur [5,7].

Schmitt [8] proposed a modification of the Kolbe reaction in which carbon dioxide introduced under pressure significantly improved the yield. For example, Baine *et al.* [9] reported obtaining 79% yield of salicylic acid at 125°C and a carbon dioxide pressure of 80–135 atm. Under these conditions, no phenol is lost and salicylic acid is obtained in an almost stoichiometric amount. This modification, known as the Kolbe–Schmitt reaction, remains the standard method for preparing a wide variety of hydroxy aromatic acids.

In the present-day industrial process for manufacturing salicylic acid, the reaction takes place in the gas–solid phase. Dry sodium phenoxide is contacted with carbon dioxide at 5 atm and temperatures up to 100°C. After absorption of approximately one molar equivalent of carbon dioxide, the temperature is raised and held at 150–160°C for several hours. One of the practical challenges in carrying out the Kolbe–Schmitt reaction in the solid phase is the difficulty of achieving absolutely anhydrous conditions and maintaining the metal aryloxide in a finely divided state. Agglomeration of particles during carbonation and inefficient mixing leads to less than optimal yields and local overheating with formation of undesirable

---

*Corresponding author. Email: achenie@engr.uconn.edu

Molecular Simulation
ISSN 0892-7022 print/ISSN 1029-0435 online © 2006 Taylor & Francis
http://www.tandf.co.uk/journals
DOI: 10.1080/08927020600615000

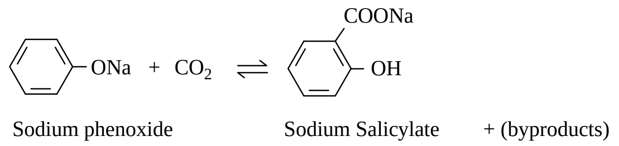

Figure 1. Kolbe–Schmitt reaction.

by-products. The reaction mixture is either a powdery solid or a viscous liquid (paste) and much effort has been made to improve the reactor design for better stirring of the reaction mixture and for enhancing the contact surface between the reactants. The use of an inert solvent or suspension medium may overcome these difficulties by facilitating a homogeneous reaction mixture, improving the stirring of the reaction mixture and in a number of cases, enabling the reaction to be carried out under milder conditions [5]. In addition, the Kolbe–Schmitt process can be carried out continuously in a suitable medium [10] eliminating the requirement of batch processes.

1.1 Background on reaction mechanism

Despite great efforts and numerous hypotheses proposed to elucidate the Kolbe–Schmitt reaction mechanism, this subject still remains unresolved. Early researchers suggested that the reaction occurs via an intermediate complex “sodium phenyl carbonate” ($PhO\cdot CO_2Na$) that forms at room temperature [6,8]. Hessler [11], citing Tijmstra [12], asserted that the complex formed between CO_2 and PhONa is not “phenyl sodium carbonate”, because this species readily looses carbon dioxide at 120°C. Tijmstra assumes a simple addition of carbon dioxide to sodium phenoxide, forming a “phenyl sodium-σ-carbonic acid” (Ph(ONa)·COOH). It has been shown that the initial chelate rearranges with the formation of a cyclic intermediate, followed by hydrogen atom migration in the synthesis of ortho substituted products [13,14]. Gilman [15] proposed a different mechanism involving phenyl sodium carbonate and metallated compounds.

As the technology evolved over the years, novel measurement tools helped detection of chelate complexes. Hales *et al.* [16], using infrared absorption spectra, found evidence of formation of a weak chelate complex between PhONa and CO_2 ($PhONa\cdot CO_2$). It was showed that this complex dissociates into the original reactants at low pressure (atmospheric or sub-atmospheric pressure) when temperature is raised to 80°C, however, it does not dissociate under the conditions of the Kolbe–Schmitt reaction at 120–160°C when pressure exceeds 4 atm. This study shows that, upon thermal activation, the chelate complex suffers an intramolecular rearrangement followed by displacement of the ortho hydrogen by electrophilic attack. Hales *et al.* excluded ortho metallated aryloxides and dimetallated intermediates from the reaction mechanism, explained by the absence of disodium salicylates products.

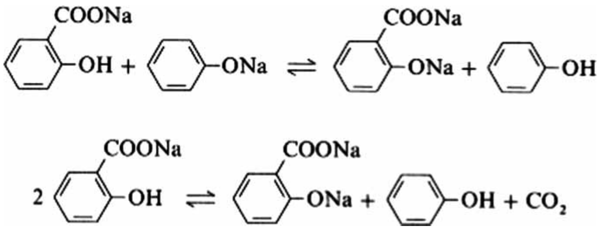

Figure 2. Side reactions.

Ayres [17] demonstrated that the chelate complex further rearranges into a π-complex with C-alkylation in the ortho position, followed by proton transfer to the phenolic oxygen. Ayres also showed that the chelate decomposes into CO_2 and PhONa on addition of solvents (such as acetone, known to form complexes with phenoxides). Experimental investigation [18] of the structure of solvent free sodium phenoxide by means of FT-IR and DTA, points to the presence of the $PhONa\cdot CO_2$ complex, as well as a further intermediate. They inferred that direct carboxylation could be excluded from the Kolbe–Schmitt reaction mechanism.

More recently [19], it has been shown that the reaction proceeded by direct carboxylation of the aromatic ring and that the $PhONa\cdot CO_2$ complex was not an intermediate in this process. Thus, chelate formation constitutes a competing reaction with the formation of salicylic or *p*-hydroxybenzoic acid. Their studies focused mainly on the carbonation of potassium phenoxide and an exact mechanism based on their hypothesis has not been presented.

Markovic *et al.* [20] performed theoretical quantum mechanical density functional theory (DFT) calculations using the Gaussian 98 suite of programs [21] and proposed a complete mechanism including three intermediates and three transition states as follows:

$$\mathrm{PhONa} + \mathrm{CO_2} \rightarrow \mathrm{B} \rightarrow \mathrm{TS1}(o - \mathrm{TS1},\, p - \mathrm{TS1}) \rightarrow \mathrm{C}$$

$$\rightarrow \mathrm{TS2} \rightarrow \mathrm{D} \rightarrow \mathrm{TS3} \rightarrow \text{Sodium salicylate (E)}$$

It was shown that $PhONa\cdot CO_2$ chelates as the first intermediate (species **B**), showing that carbon dioxide can only attack at the –O–Na site. The chelate undergoes intramolecular rearrangement, followed by electrophilic attack with displacement of the *ortho* hydrogen atom. Intermediate **C** exhibits a similar structure to that of the chelate complex suggested by Hales *et al.* [16]. Markovic’s study also provides a quantitative explanation for the low yields of *p*-hydroxybenzoic acid by-product and the equilibrium behavior of the Kolbe–Schmitt reaction.

In this work, we investigate the effects of some of the solvents identified in the literature on the mechanism of this reaction. We also aim to identify new or alternative solvents that may enhance the reaction conversion and create a homogeneous reaction mixture, thereby improving contact surface between reactants, heat transfer and product quality. To accomplish these objectives, we propose a three-step methodology: (1) DFT calculations to validate the reaction mechanism; (2) design of alternative solvents using a computer aided molecular design (CAMD) technique and solvation calculations and finally; (3) estimation of the rate constants using transition state theory and kinetic analysis. The third step has been discussed in a paper submitted elsewhere [22] and is therefore not addressed in this paper.

1.2 Density functional theory

DFT methods represent one of the classes of electronic structure methods that have come into wide use. These methods are similar to *ab initio* methods in many ways. DFT calculations require about the same amount of computational resources as Hartree–Fock theory, the least expensive *ab initio* methods. DFT methods are attractive because they include the effects of electron correlations, i.e. the fact that electrons in a molecular system react to one another's motion and attempt to keep out of one another's way in their model. Hartree–Fock calculation considers this effect only in an average sense, i.e. each electron sees and reacts to an averaged electron density. Methods that include electron correlations account for the instantaneous interactions of pairs of electrons with opposite spin. This approximation causes Hartree–Fock results to be less accurate for the same types of system. Thus, DFT methods can provide the benefits of some more expensive *ab initio* methods at essentially Hartree–Fock cost.

2. Validation of the Kolbe–Schmitt reaction mechanism

To confirm the mechanism proposed by Markovic *et al.* [20], quantum mechanical calculations were performed using the Jaguar 4.2 suite of programs [23]. DFT calculations, geometry optimization and transition state search for the different structures along the reaction path were conducted at B3LYP level of theory and all the atoms were described by LAV3P** basis set [24]. After a series of tests with LAV2D**, LACVP**, LAV3P** and LAV3P**++ basis sets, LAV3P** was finally selected for the calculations, taking into account the trade-off between accuracy and computational effort. Although both LAV3P** and LAV2D** basis set use double zeta to approximate the valence orbital, still LAV3P** basis set is more accurate than LAV2D**, because LAV3P** uses 6–31 G for all non-ECP's and the latter uses D95V basis for all non-ECP's. Whereas the LACVP** results were very different from those reported by Markovic *et al.* [20] because calculations that use LACVP** basis set use LACVP effective core potentials for some atoms and LAV3P effective core potentials or 6–31 G basis function (with or without the use of polarization function options) for other atoms, offering no possibility for comparison. Also, in comparison to 6–31 G** (used as a default in Jaguar 4.8 suite of programs), the LAV3P** can describe atoms such as sodium (Na) better. Moreover, LAV3P** and LANL2DZ (used in Markovic *et al.*) are both electron core potential (ECP) basis sets and therefore provide the same platform for comparison of results. Adding the two diffused functions (LAV3P**++ basis set) did not notably modify the results; however the computational effort increased significantly. The calculations performed using LAV3P** were robust and reproducible, the average CPU time being around 6200 s for the geometry optimization calculations and around 9900 s for the transition state searches, using a single node of a Beowulf Linux Cluster (with the Athlon™ MP 1800+ at 1.53 GHz).

Calculations were performed for normal conditions (0°C and 1 atm) to compare with the results obtained by Markovic *et al.* [20]. Optimized geometries and transition states are presented in figure 3. Starting from reactants placed in the workspace relatively far from each other and optimizing this initial geometry (varying the distances and angles), complex **B** is obtained as the optimized structure, having the lowest energy around the initial geometry. Also, intermediate **C** was obtained as the optimized structure if the initial reactants were placed relatively close to each other such that direct substitution would be the most probable; however, there is no indication that direct substitution is plausible in this situation. No new C–C bond in *ortho* or *para* position in a structure with low-energy around this initial geometry appears after optimization. Based on a HOMO–LUMO analysis, Markovic *et al.* deduce that the reactive site in the first step is the O–Na bond. Our investigations showed that the initial chelate formation is likely to occur, since CO_2 is a weak electrophile and the O–Na bond is highly polarized. In addition, this mechanism is verified by an examination of charges on the *ortho* C atom in sodium phenoxide and on the C atom in CO_2 compared with the charges on the same atoms in complex **B**. The *ortho* position in the aromatic ring has a partial charge of -0.45467 in PhONa and of -0.37888 in complex **B**. The C atom in CO_2 has a partial charge of $+0.63824$, while in complex **B** the charge is $+0.90266$. Therefore the chelate formation facilitates the subsequent electrophilic attack and the reaction is more likely to follow this mechanism than direct carboxylation.

The energy profile along the reaction path follows the same pattern as that reported by Markovic *et al.* [20] (figure 4), however the energies obtained using the LAV3P** basis set in Jaguar 4.2 have a small average percentage error of 1.5% in comparison to the energies obtained by Markovic *et al.* We expect that the small error can mostly be attributed to the differences between the LANL2DZ basis set in the Gaussian 98 suite of programs, used in Markovic's work and LAV3P** in the Jaguar 4.2 suite of programs, used in this work. The difference can also be associated with the way Gaussian 98 and Jaguar 4.2 calculate electrostatic potentials for various species. The values for each species in the reaction are shown in table 1.

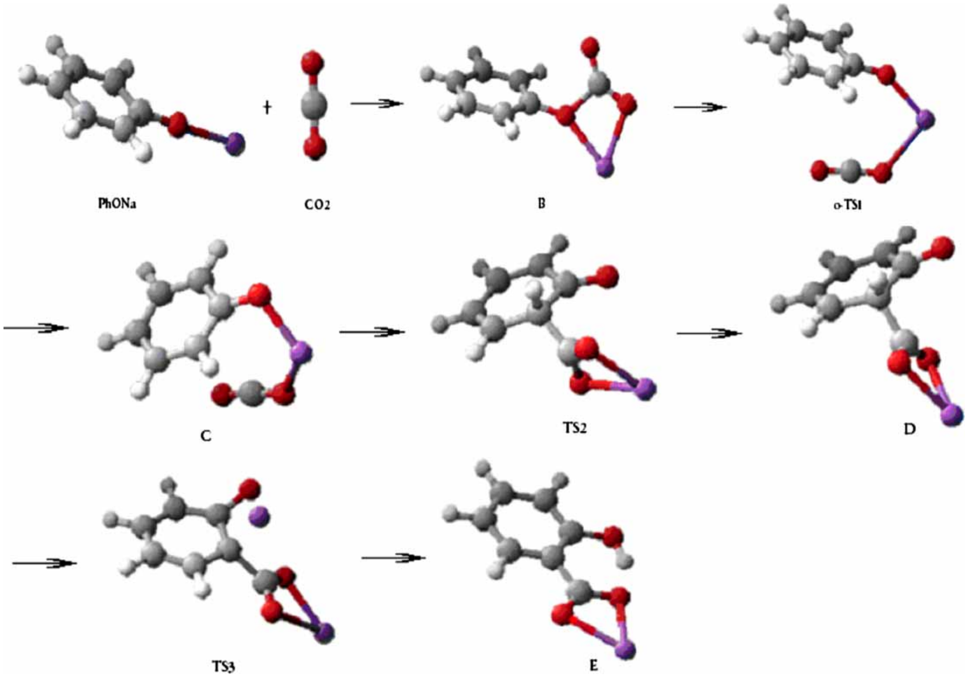

Figure 3. The Kolbe–Schmitt reaction mechanism. The ground states are the optimized geometries obtained using B3LYP level of theory and atoms described by LAV3P** basis set. The transitions states geometries were found using the transition state search option in Jaguar 4.2, starting from the optimized structures of the reactants and products. The labels of the structures along the reaction path (intermediates and transition states) are the same as Markovic's notations (Markovic *et al.* 2002). The atoms in grey are carbon atoms, white are hydrogen, red are oxygen and purple are sodium (reproduced from Stanescu *et al.* [22]).

For the structures along the reaction path, the calculated thermodynamic properties, namely heat capacity, enthalpy, entropy and Gibbs free energy of the molecules are shown in table 2. With a confirmed reaction mechanism, we were able to calculate the same set of properties for the Kolbe–Schmitt reaction conducted, in the presence of solvents.

3. Effect of solvents on the Kolbe–Schmitt reaction

3.1 Reported solvents for the reaction

A wide variety of organic compounds have been reported as solvents or suspension media for the Kolbe–Schmitt reaction. An obvious choice of solvent would be water, since it dissolves the alkali metal aryloxides. However,

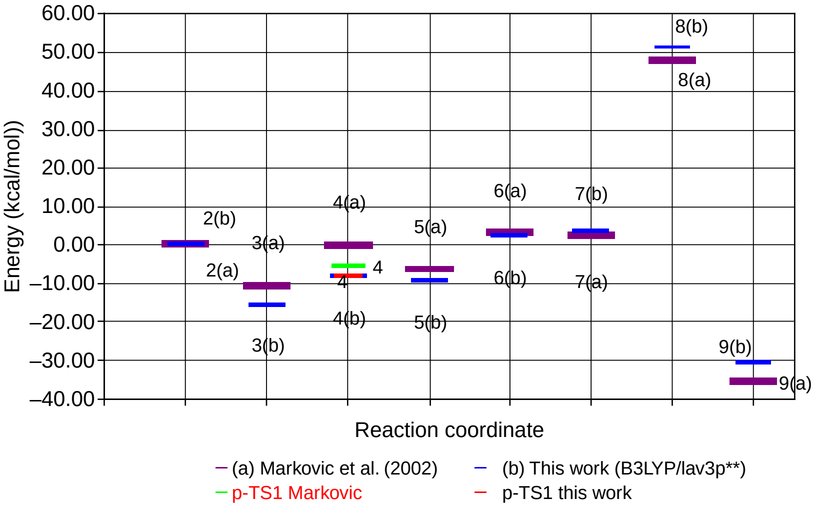

Figure 4. Potential energy diagram. The maroon dash represents the energies of different structures along the Kolbe–Schmitt reaction path reported by Markovic *et al.* (2002). The blue dash represent the energies of the optimized structures and transition states calculated in this work at B3LYP/LAV3P** level of theory. Notations: 2—Reactants; 3—Intermediate **B**; 4—Transition state TS1; 5—Intermediate **C**, 6—Transition state TS2; 7—Intermediate **D**; 8—Transition state TS3; 9—Product **E**.

Table 1. Energy values obtained from Jaguar 4.2 compared with Markovic *et al.*

Structure	*Position on the reaction path*	*Markovic et al. (kcal/mol^{-1})*	*Current work (kcal/mol^{-1})*
CO_2		−118308.9247	−118334.3541
PhONa		−192685.7222	−192707.6107
Reactants (A)	2	−310994.6469	−311041.9647
B	3	−311005.5629	−311057.7137
o-TS1	4	−310995.1846	−311050.2785
p-TS1	4′	−311000.1143	−311050.214
C	5	−311001.3373	−311051.4894
TS2	6	−310991.8451	−311039.9471
D	7	−310992.5015	−311038.8572
TS3	8	−310946.8345	−310990.5258
E	9	−311030.2054	−311072.7613

water inhibits the carbonation of monohydric phenols and therefore it should be removed from the reactants prior to reaction. This adverse effect may be due to strong chelation of water molecules with alkali metal aryloxides, preventing the initial addition of carbon dioxide. Another reason may be the hydrolysis of the alkali salt to phenol and sodium hydroxide. Subsequently, introducing carbon dioxide leads to the formation of sodium bicarbonate, the phenol remaining unchanged [5]. Hydrocarbons are among the most common solvents, but they generally may be used only as suspension media in the Kolbe–Schmitt reaction since metal aryloxides often are not soluble in this type of solvent. Moseley [25] reported xylene as suspension media for the reaction conducted continuously, while Ueno [26] identified kerosene, light oil and gasoline as dispersants.

A series of other possible solvents have been identified in the literature. The Kolbe–Schmitt reaction can be performed in excess phenol [27–29]. Barkley [30] presented a series of experiments carried out in the presence of higher alcohols (e.g. isooctanol, isodecyl alcohol) and carbonation of metal aryloxides in cyclic diethers (dioxane, pyridine and quinoline) has also been reported [5]. Hirao *et al.* [31] used aprotic polar solvents such as DMF and DMSO as solvents for carboxylation of phenol derivatives, enabling the reaction to be homogeneous at 100–180°C. Kunert *et al.* [18] investigated the structure of sodium phenoxide crystals and its complexes with THF and TMU (*N*,*N*,*N*′,*N*′-tetramethyl urea). Furuya *et al.* [32] proposed a process for preparing hydroxybenzoic acids by using a mixture of alkali metal compound, phenol and an aprotic polar solvent (amides, dimethyl sulfoxide or sulfolane). Although these are all potential solvents, we did make computations for these cases.

Table 2. Thermodynamic properties for the optimized structures and transition states in the Kolbe–Schmitt reaction at 150°C and 4 atm. Results from DFT calculations using Jaguar 4.2 (reproduced from Stanescu *et al.* [22]).

Structure		*S* *(cal/mol^{-1} K^{-1})*	*H* *(kcal/mol^{-1})*	*G* *(kcal/mol^{-1})*
CO_2		51.7477	3.4495	−18.4475
PhONa		93.5705	9.0783	−30.5160
Reactants (A)	2	145.3182	12.5278	−48.9635
B	3	111.8003	12.1358	−31.1725
o-TS1	4	119.5505	13.2716	−37.3162
p-TS1	4′	120.1996	13.2837	−37.5787
C	5	113.3663	12.4217	−35.5493
TS2	6	108.6233	12.1929	−33.7752
D	7	112.9425	12.1539	−35.6377
TS3	8	110.8196	12.6106	−34.2827
E	9	106.6856	11.5445	−33.5995

Additional solvents proposed in literature provided the focus for solvation calculations presented in this work. Wideqvist [33] showed that alkali salicylates are readily soluble in acetone, ethanol and methanol. Glycols (ethylene glycol, glycerol) and 1-butanol have also been used as solvents for the Kolbe–Schmitt reaction. Glycerol has been employed as a solvent for carbonations at atmospheric pressure, when the reaction mixture is heated at 130–210°C with alkali bicarbonate in a stream of carbon dioxide. Fry [34] suggested lower dialkyl ketones (insoluble in water) as solvents for alkali phenolates and conducted the Kolbe–Schmitt reaction for sodium phenoxide in diisobutyl ketone. With sodium phenoxide as the starting reactant, data using these solvents are summarized in table 3.

The yields of salicylic acid achieved by using these solvents are significantly lower (in some cases no product was obtained) in comparison with the current solvent-free Kolbe–Schmitt reaction, which gives up to 97% yield. As posited by Isemer, cited by Lindsey and Jeskey [5], the data show that carbonation proceeds most readily in solvents having low dielectric constants.

3.2 Solvent design

In addition to solvents identified in the literature, a systematic CAMD algorithm was employed to find new/alternative solvents that may exhibit better performances in this reaction. The CAMD algorithm utilizes functional group information to generate structures (molecules) and applies a group-contribution method to estimate the properties of the designed compounds, which are then evaluated with respect to the specified set of desired properties. Thus, this methodology leads to the identification of solvents having desired types and properties. Some of the most important contributions to

Table 3. Carbonation of sodium phenoxide in various solvents (adapted from Lindsey and Jeskey 1957).

Solvent	*Dielectric constant*	*Temperature (°C)*	*Pressure (atm)*	*Salicylic acid yield (%)*
Methanol	31.2	140	22	No product
Ethanol	25.8	140	6	No product
1-Butanol	19.2	155	10	7.5
Glycol	41.2	140	6	No product
Glycerol	56.2	170	10	No product
Xylene (suspension)	2.6	138	1	33.5
Diisobutyl ketone	–	150	1	18.9

this approach of CAMD have been presented by Gani *et al.* [35], Venkatasubramanian *et al.* [36], Constantinou *et al.* [37], Duvedi and Achenie [38], Churi and Achenie [39], Marcoulaki and Kokossis [40], Harper and Gani [41] and Wang and Achenie [42]. In this study, we used ProCAMD version 1.41 tool within the integrated computer aided system (ICAS) version 7.0 [43].

The design of solvents to be used in the Kolbe–Schmitt reaction takes into account several criteria, which translate into a set of desired properties applied as constraints in the selection of the feasible alternatives. The candidate solvents were designed to have specific types such that they are inert toward the reaction components (reactants and products). Substances such as acids and halogenated compounds were excluded due to their potential reactivity toward the alkali metal aryloxides. Amines were also excluded due to their potential toxicity, which is undesirable in a pharmaceutical process. Additionally, the candidate solvents must be liquid under the reaction conditions; therefore their melting and boiling point become property constraints in the design procedure.

Since organic salts such as metal aryloxides and salicylates are not present in common databases and their properties not readily available or easy to predict (e.g. solubility parameter), the characteristics of mixtures between these compounds and the designed solvents are difficult to estimate (miscibility, solvent power, selectivity etc.). However, according to the simple solubility parameter theory, it is assumed that if the solubility parameter of a solvent is around the same value to that of the solute, they will be miscible (“like dissolves like”). The product sodium salicylate was selected as the solute. Therefore a solvent with high solubility for this compound will stabilize it within the reaction mixture, thereby improving its yield. Taking into account the solubility parameter of sodium salicylate reported by Barra *et al.* [44] to be 30.81 $(\mathrm{MPa})^{1/2}$, the candidate solvents must have a solubility parameter around the same value. It is also known that water is a good solvent for sodium salicylate, therefore the solubility parameter limits considered for solvent design were between 30 and 48 $(\mathrm{MPa})^{1/2}$.

The resulting design criteria are as follows:

- Types of compounds: acyclic, aromatic and cyclic alcohols, phenols, aldehydes, ketones, ethers and esters, compounds containing double and triple bonds;
- Compounds can contain 2–10 groups, 0–3 functional groups, 0–3 same functional groups;
- Solvents contained in ProCAMD common solvent database were also included; as user specified compounds;
- Melting point: $T_m < 420\,\mathrm{K}$;
- Boiling point: $T_b > 425\,\mathrm{K}$;
- Total solubility parameter: 30–48 $(\mathrm{MPa})^{1/2}$ (target value 31 $(\mathrm{MPa})^{1/2}$).

Additionally, partial solubility parameters were estimated in the solvent design step and included in an analysis based on the Teas graph presented in figure 5. A simple method to visualize potentially suitable solvents for a particular substance is to place them on a triangular diagram (Teas graph) according to their Hansen partial solubility parameters: δ_H, δ_D, δ_P [45]. For sodium phenoxide, according to Barra *et al.* [44], the partial solubility parameters determined empirically are: $\delta_H = 16.58$ $(\mathrm{MPa})^{1/2}$, $\delta_D = 16.55$ $(\mathrm{MPa})^{1/2}$, $\delta_P = 20.01$ $(\mathrm{MPa})^{1/2}$ (point marked 1 in figure 5). The same study presented another set of partial solubility parameters, calculated using a group contribution method: $\delta_H = 20.16$ $(\mathrm{MPa})^{1/2}$, $\delta_D = 21.18$ $(\mathrm{MPa})^{1/2}$, $\delta_P = 11.23$ $(\mathrm{MPa})^{1/2}$ (point marked 1$*$ in figure 5). The solubility region is determined approximately by drawing a contour around the solute in the Teas diagram. In this case, the contour was sketched such that water is included inside the solubility region. Compounds situated in the close vicinity of the solute are the most likely to dissolve it. It can be observed from figure 5 that glycols, alcohols and dihydroxy aromatic compounds are among the suitable solvents for sodium phenoxide, which confirms the results from the solvent design step and is consistent with the solvents reported in the literature.

Molecular weight and liquid density are input data required by the solvation calculations as solvent specifications; hence these properties are also evaluated during the solvent design runs. The dielectric constant is also an input parameter in Jaguar 4.2 solvation calculations; however this property is not available in ProCAMD. Consequently, dielectric constants were estimated using ProPred 3.6 tool within ICAS [43], based on Constantinou and Gani group-contribution technique [37].

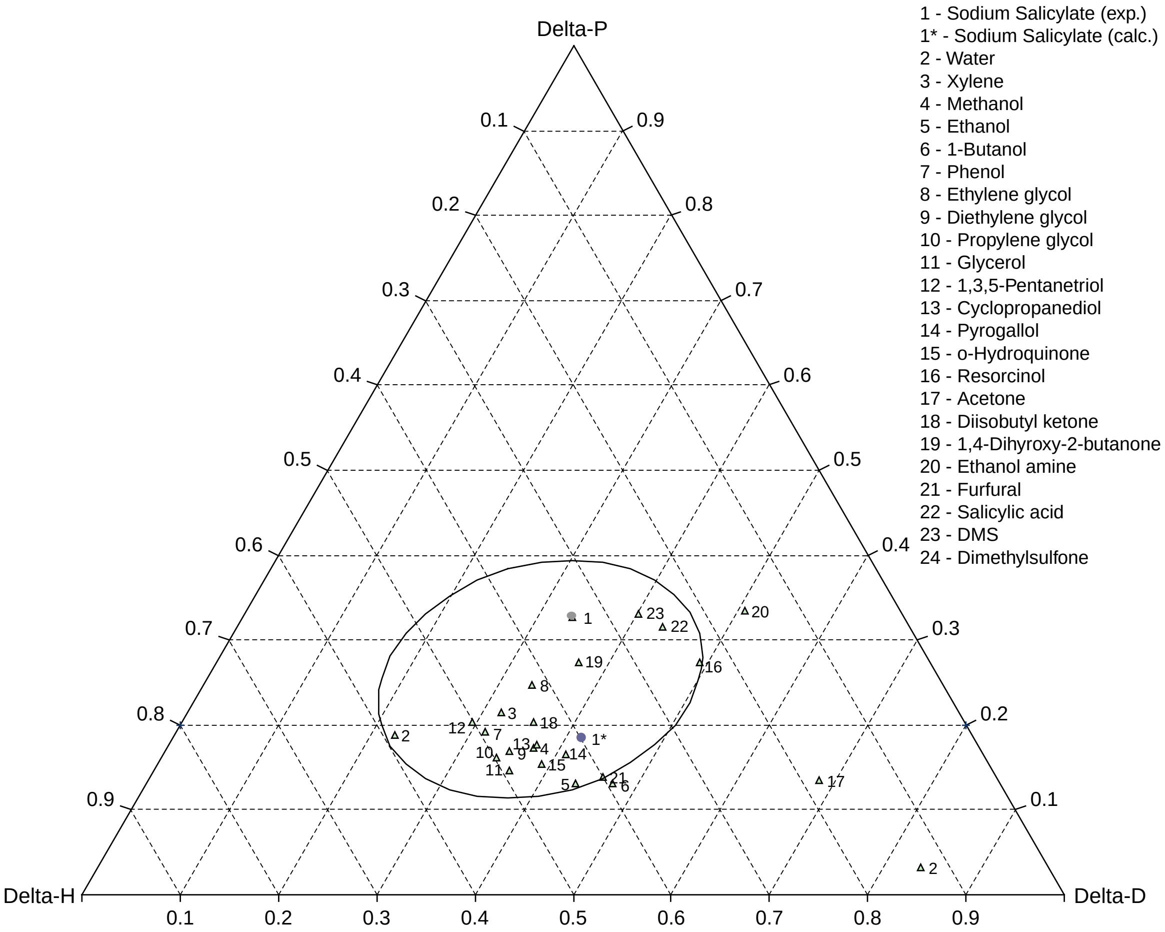

Figure 5. Teas graph based on Hansen partial solubility parameters (reproduced from Stanescu *et al.* [22]).

The results from the solvent design step are presented in table 4.

All the acyclic compounds are listed together with their properties. Only one example of the cyclic compounds and two examples of the aromatic compounds are given since these compounds cannot be found in common databases, making their properties unavailable and difficult to estimate, in particular their dielectric constants. The cyclic compounds designed contain 2–3 hydroxyl groups or 2 hydroxyl groups and a carbonyl group, placed around small rings (3–4 carbon atoms). These cyclic compounds are likely to be strained and possibly unstable under the reaction conditions. The aromatic compounds contain 2–3 hydroxyl groups or 2 hydroxyl groups and a carbonyl or carboxylic group, their functionalities being similar to those of acyclic or cyclic compounds. Aromatic compounds are oftentimes toxic, hence undesirable in a pharmaceutical process. Considering these factors, only the acyclic compounds were further analyzed with respect to their effects on the Kolbe–Schmitt reaction.

3.3 *Solvation calculations*

The effect of each solvent on the geometries along the reaction path was investigated by specifying the solvent dielectric constant, molecular weight and density in the Jaguar 4.2 suite of programs. Jaguar 4.2 [23] uses a self-consistent reaction field (SCRF) method and a Poisson–Boltzmann solver [46,47] to describe solvated structures. The SCRF method in Jaguar 4.2 first calculates the gas phase wave function and uses that information to obtain electrostatic potential. It then fits the electrostatic potentials into a set of atomic charges that are passed to the Poisson–Boltzmann solver. The Poisson–Boltzmann solver represents the solvent as a continuum of uniform dielectric constant, a layer of charges around the molecular surface and determines the reaction field from the atomic charges. The solvent point charges thus derived are used in a new quantum mechanical wave function calculation, repeating this procedure until self-consistency is achieved.

Solvation energies were computed for minimum-energy solvated structures and solvated transition states (table 5). Thus, the ground states (reactants, product and intermediates) were optimized in solution, while for the solvated transition states only single point energy calculations were performed due to the considerable computational effort. For example, when 1,2-ethanediol is used as solvent, the average CPU time for energy-minimization of the ground states in solution was approximately 22,700 s, 3.6 times the CPU time needed for the gas phase optimization. For the single point energy calculations of the solvated transition states, the average CPU time was approximately 20,400 s, while transition state searches would require 30–50 iterations to converge.

Solvation calculations were performed with density functional methods using solvents reported in the literature (table 3) and the designed candidate solvents for which the necessary data were available (table 4). The energies for each solvated structure along the reaction path are presented in table 5 and the results are graphically presented in figure 6.

The results shows that the energies for all the solvated geometries are lower than that for the same structures in the absence of solvent, demonstrating that the solvents stabilize the species along the reaction path. As expected, polar solvents have greater impact on the reactive species' energies (table 5), thermodynamic properties and solvation energies (table 6). In the cases where solvents have low dielectric constants, the differences in potential energy are less significant, indicating that the structures along the reaction path are less stable in these solvents. However, a solvent's performance is determined by its ability to increase the rate constant, to displace the equilibrium towards the product and/or to improve mass transfer. The rate constant calculations and analysis have been discussed in a paper submitted elsewhere [22] and are therefore not addressed in this paper.

Table 4. Candidate solvents using ProCAMD (reproduced from Stanescu *et al.* [22]).

Designed solvent	*Solubility parameter ($MPa^{1/2}$)*	δ_H ($MPa^{1/2}$)	δ_D ($MPa^{1/2}$)	δ_P ($MPa^{1/2}$)	*Normal melting point (K)*	*Normal boiling point (K)*	*Molecular weight (kg/kmol)*	*Liquid density (kg/dm^3)*	*Dielectric constant*
Acyclic Compounds: number of compounds designed: 11711; number of compounds selected: 9; total time used to design: 0.85 s									
1,3-Propylene glycol	30.51	23.51	17.00	9.77	235.53	453.47	76.09	1.05	33.68
Compound 2: $2CH_3$ $1CH_2$ 1CH 1C 3OH	30.70	24.42	17.39	8.61	274.95	527.88	120.15	1.19	32.99*
Compound 3: $1CH_3$ $2CH_2$ 2CH 3OH	30.85	24.27	17.19	8.51	268.97	533.19	120.15	1.18	32.37*
Compound 4: $1CH_3$ $3CH_2$ 1C 3OH	31.16	24.47	17.86	8.64	281.91	533.25	120.15	1.20	34.17*
1,3,5-Pentanetriol	31.30	24.33	17.65	8.54	276.33	538.42	120.15	1.18	33.36*
1,4-Dihydroxy-2-butanone	31.37	22.35	18.07	12.43	275.35	510.72	104.10	1.24	35.59*
1,2,3-Butanetriol	32.86	26.50	17.33	10.14	261.87	518.82	106.12	1.24	34.10*
Glycerol (1,2,4-butanetriol)	33.37	26.57	17.89	10.19	269.74	524.43	106.12	1.25	37.62*
1,2-Ethanediol	33.48	26.74	17.16	12.64	225.56	431.87	62.07	1.11	37.7
Cyclic compounds: number of compounds designed: 122866; number of compounds selected: 10; total time used to design: 14.64 s									
1,2-Cyclopropanediol	34.40	27.28	15.81	13.15	223.12	438.77	74.08	1.38	†
Aromatic compounds: number of compounds designed: 3416848; number of compounds selected: 41; total time used to design: 39.82 s									
o-Hydroquinone (1,2-benzenediol)	30.10	16.82	20.04	8.01	371.39	592.30	180.20	1.24	†
Pyrogallol (1,2,3-benzenetriol)	30.94	17.32	20.50	8.21	371.39	603.67	180.20	1.24	†

[*] Estimated using ProPred 3.6. [†] Dielectric constants not available. Difficulties in estimating their values.

4. Discussion and conclusions

A theoretical methodology was proposed to study the effects of solvents on the Kolbe–Schmitt reaction. DFT calculations at the B3LYP/LAV3P** level of theory were performed and the results supported Markovic's four-step reaction mechanism [20]. The results give a theoretical justification for empirical results reported in the literature, confirming Isemer's suggestion that solvents having low dielectric constant are more suitable for the carbonation of alkali metal aryloxides. Infact, when low dielectric constant compounds are used as the reaction media, the reaction primarily takes place in suspension and the solvent acts as a diluent.

The solvents used in the study, were first identified/designed through a CAMD technique; the solvents were capable of creating a homogeneous reaction mixture, while at the same time promoting the reaction. The most important design criteria were considered to be the solubility parameter, together with the melting and boiling points, selected such that the solvent is liquid under the reaction conditions. The results from the design step revealed that compounds containing 2–3 hydroxyl groups or 2 hydroxyl groups and a carbonyl or carboxyl group were potentially suitable solvents for

Table 5. Energy of the solvated geometries (kcal mol^{-1}).

Structure/solvent	*Diisobutyl ketone*	*1,3-propylene glycol*	*1,4-dihydroxy 2-butanone*		
CO_2	− 118338.8237	− 118338.0645	− 118338.0745		
PhONa	− 192797.084	− 192809.6508	− 192809.2036		
Reactants (A)	− 311135.9078	− 311147.7154	− 311147.2781		
B	− 311144.7964	− 311159.7657	− 311159.8052		
o-TS1	− 311117.3187	− 311127.1132	− 311127.255		
C	− 311123.5567	− 311135.281	− 311134.9144		
TS2	− 311110.612	− 311121.0269	− 311121.052		
D	− 311121.879	− 311134.8082	− 311134.621		
TS3	− 311064.113	− 311127.1132	− 311073.9965		
E	− 311147.9087	− 311159.8288	− 311159.4407		
Structure/solvent	Methanol	Ethanol	1-Butanol	Ethylene glycol	Glycerol
CO_2	− 118308.9247	− 118338	− 118337.9739	− 118337.8343	− 118338.0983
PhONa	− 192685.7222	− 192810	− 192808.0963	− 192804.6386	− 192810.5068
Reactants (A)	− 310994.6469	− 311148	− 311146.0702	− 311142.4729	− 311148.6051
B	− 311005.5629	− 311160	− 311158.3253	− 311154.5216	− 311159.9664
o-TS1	− 310995.1846	− 311128	− 311126.0802	− 311123.5564	− 311127.9309
C	− 311001.3373	− 311139	− 311134.117	− 311130.2961	− 311136.6342
TS2	− 310991.8451	− 311122	− 311119.78	− 311117.1566	− 311121.7138
D	− 310992.5015	− 311136	− 311133.3682	− 311129.5244	− 311136.0153
TS3	− 310946.8345	− 311075	− 311072.8025	− 311070.5124	− 311074.7464
E	− 311030.2054	− 311162	− 311159.4906	− 311159.4906	− 311161.7577

sodium phenoxide. Two of the designed solvents were found to be identical with compounds summarized by Lindsey and Jeskey [5]. An extensive kinetic analysis of the reaction has been done and reported in Stanescu and Achenie [22]. In the latter, we considered the reaction carried out in the presence of the designed solvents. The results demonstrated that, although the solvents were capable of dissolving the product (sodium phenoxide) and improve the reaction's rate constants; there was no improvement in product yield. This can only be explained by reaction reversibility.

Further investigations may consider estimating the effects of other types of solvents, such as aprotic polar solvents, or examining in more depth the solubility of alkali metal aryloxides, carbon dioxide and hydroxy aromatic acids salts in different media. These studies could provide the means to calculate the fraction of product that precipitates from the reaction mixture.

Acknowledgements

This material is based upon work partially supported by the National Science Foundation under Grant No. 0109928. Any opinions, findings and conclusions or recommendations expressed in this material are those of

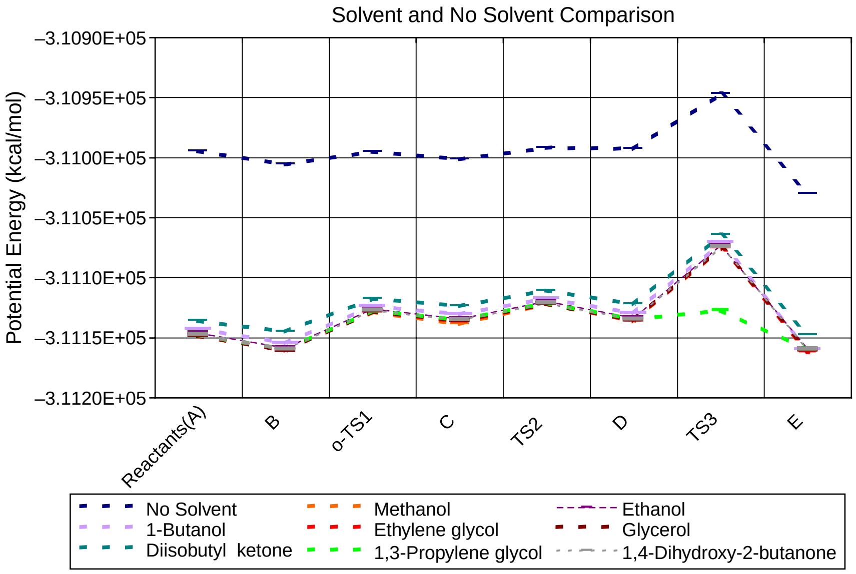

Figure 6. Energy diagram for Kolbe–Schmitt reaction in the presence of various candidate solvents.

Table 6. Thermodynamic properties of solvated structures: *S* (cal/mol K), *H* (kcal/mol), *G* (kcal/mol) and solvation energy (kcal/mol). Results from DFT calculations (reproduced from Stanescu *et al.* [22]).

Solvent			*Methanol*	*Ethanol*	*1-Butanol*	*Ethylene glycol*	*Glycerol*	*1,3-Propylene glycol*	*1,4-Dihydroxy-2-butanone*	*Diisobutyl ketone*
Structure										
CO_2		S	51.7885	51.7900	51.7849	51.7911	51.7871	51.1910	51.7879	51.7823
		H	3.4599	3.4603	3.4590	3.4605	3.4595	2.2589	3.4597	3.4584
		G	− 18.5444	− 18.4547	− 18.4538	− 18.4549	− 18.4542	− 13.0037	− 18.4543	− 18.4533
		SE	− 2.6811	− 2.6248	− 2.5607	− 2.6825	− 2.6888	− 2.6669	− 2.6714	− 2.4433
PhONa		S	90.6425	87.3172	87.2947	90.3582	87.6886	90.4726	87.4746	93.1803
		H	9.3035	9.9472	9.3352	9.2658	9.3959	9.2623	9.3656	9.1299
		G	− 29.0519	− 27.6010	− 27.6035	− 28.9693	− 27.7096	− 29.0212	− 27.6493	− 30.2994
		SE	− 49.4639	− 48.5127	− 47.0230	− 49.5298	− 49.3421	− 49.1841	− 49.0455	− 43.7396
Reactants (A)	2	S	142.431	139.107	139.080	142.149	139.476	141.664	139.263	144.963
		H	12.763	13.408	12.794	12.726	12.855	11.521	12.825	12.588
		G	− 47.596	− 46.056	− 46.057	− 47.424	− 46.164	− 42.025	− 46.104	− 48.753
		SE	− 52.145	− 51.138	− 49.584	− 52.212	− 52.031	− 51.851	− 51.717	− 46.183
B	3	S	110.3060	109.8415	113.8361	107.9298	109.2169	112.0213	111.8203	115.3116
		H	12.2233	12.2237	12.1826	12.1028	12.2000	12.3189	12.3089	12.2422
		G	− 34.4526	− 34.2557	− 35.9871	− 33.5677	− 34.0151	− 35.0829	− 35.0079	− 36.5519
		SE	− 47.8947	− 47.2821	− 45.4546	− 47.8581	− 48.0195	− 47.8763	− 47.8941	− 41.7096
o-TS1	4	S	118.3279	113.3600	113.9970	113.2606	119.5554	113.2751	119.2694	114.5049
		H	13.4270	13.4836	13.5112	13.4797	13.4973	13.4864	13.4897	13.5150
		G	− 36.6435	− 34.4846	− 34.7267	− 34.4466	− 37.0926	− 34.4028	− 36.9791	− 34.9377
		SE	− 39.9398	− 38.9191	− 37.7602	− 39.7736	− 39.7270	− 39.4028	− 39.4709	− 34.8453
C	5	S	117.1783	116.9158	115.1133	114.8351	113.4456	120.0099	113.6554	117.8421
		H	13.7294	13.4825	13.2249	13.3069	13.5344	13.3228	13.3457	13.3832
		G	− 35.8547	− 35.9905	− 35.4853	− 35.2856	− 34.4701	− 37.4594	− 34.7476	− 36.4817
		SE	− 41.8175	− 39.8910	− 38.3077	− 41.0043	− 40.9159	− 37.4594	− 44.9701	− 35.4838
TS2	6	S	106.7144	103.0480	107.2198	106.9896	107.7994	106.7971	107.4585	106.7998
		H	12.3921	12.4595	12.4068	12.4048	12.4202	12.3948	12.4127	12.3933
		G	− 32.7641	− 31.1453	− 32.9633	− 32.8679	− 33.1951	− 32.7964	− 33.0584	− 32.7990
		SE	− 42.5969	− 41.6567	− 40.4230	− 42.5576	− 42.5048	− 42.2387	− 42.2401	− 37.3509
D	7	S	110.7770	111.5654	111.0622	109.9111	116.0556	110.9953	116.6646	115.2498
		H	12.4580	12.4856	12.5062	12.4036	12.4948	12.4934	12.5035	12.4388
		G	− 34.4172	− 34.7234	− 34.4898	− 34.1053	− 36.6184	− 34.4743	− 36.8631	− 36.3292
		SE	− 46.8171	− 45.5436	− 44.1130	− 46.6422	− 46.4876	− 46.2548	− 50.1413	− 40.8395
TS3	8	S	109.0687	109.0722	108.8412	108.7968	109.4836	113.2751	109.1734	108.4086
		H	12.8274	12.8357	12.7996	12.8176	12.8376	13.4864	12.8264	12.7884
		G	− 33.3250	− 33.3182	− 33.2565	− 33.2198	− 33.4904	− 34.4478	− 33.3703	− 33.0847
		SE	− 43.0795	− 42.0951	− 41.0593	− 42.9949	− 42.9257	− 39.4028	− 42.6551	− 38.0478
E	9	S	113.2792	110.2593	110.2593	111.2801	111.6464	112.2988	113.2596	109.6898
		H	11.9969	11.8862	11.8862	11.9568	12.0450	12.0146	12.0476	11.8838
		G	− 35.9372	− 34.7700	− 34.7700	− 35.1313	− 35.1982	− 35.4047	− 35.8783	− 34.5314
		SE	− 43.6725	− 42.7294	− 42.7294	− 43.6572	− 43.1593	− 42.8357	− 46.4474	− 37.6761

the authors and do not necessarily reflect the views of the National Science Foundation. The authors would also like to thank Dr Rafiqul Gani's group at CAPEC (Department of Chemical Engineering, Technical University of Denmark) for allowing us to use ICAS for the solvent design section of this study.

Notation

ΔG	Gibbs free energy of reaction, $\mathrm{kcal\,mol^{-1}}$
ΔH	Enthalpy of reaction, $\mathrm{kcal\,mol^{-1}}$
ΔS	Entropy of reaction, $\mathrm{cal\,mol^{-1}\,K^{-1}}$
G	Free Gibbs energy, $\mathrm{kcal\,mol^{-1}}$
H	Enthalpy, $\mathrm{kcal\,mol^{-1}}$
h	Plank constant $= 6.626176\mathrm{E} - 34\,\mathrm{J\,s}$
k	Rate constant
k_B	Boltzmann constant $= 1.380662\mathrm{E} - 23\,\mathrm{m^2\,kg\,s^{-2}\,K^{-1}}$
R	Universal constant of gases $= 1.987\,\mathrm{cal\,mol^{-1}\,K^{-1}}$
S	Entropy, $\mathrm{cal\,mol^{-1}\,K^{-1}}$
SE	Solvation energy, $\mathrm{kcal\,mol^{-1}}$
T	Temperature, K
T_m	Melting point
T_b	Boiling point
δ_H	Hydrogen bonding component of Hansen solubility parameter, $\mathrm{MPa^{1/2}}$
δ_D	Dispersion component of Hansen solubility parameter, $\mathrm{MPa^{1/2}}$
δ_P	Polar component of Hansen solubility parameter, $\mathrm{MPa^{1/2}}$

References

[1] M.M. Chren, D.R. Bickers. Dermatological pharmacology. In *Pharmacological Basis of Therapeutics*, Goodman, Gilman (Eds.), p. 1587, Pergamon press, New York (1990).

[2] J.E.F. Reynolds (Ed.). Salicylic acid. *Martindale The Extra Pharmacopoeia*, 31, p. 1093, The Royal Pharmaceutical Society, London (1996).

[3] M. Windholz. Salicylic acid. *The Merck Index*, 10, p. 8190, Merck & Co Inc, Rahway, NJ, USA (1983).

[4] http://en.wikipedia.org/wiki/salicylate.

[5] A.S. Lindsey, H. Jeskey. The Kolbe–Schmitt reaction. *Chem. Rev.*, **57**, 583 (1957).

[6] H. Kolbe. Ueber synthese der salicylsaure. *Annales*, **113**, 125 (1860).

[7] T. Rieckmann. Salicylic acid. Fachhochschule Köln, University of Applied Sciences Cologne, Department of Plant Design and Chemical Engineering, MEng/reaction kinetics (www.av.fh-koeln.de/professoren/rieckmann/chemischeprozesstechnik/lab_na-phenolate/na-phenolate.html) (2004).

[8] R. Schmitt. Beitrag zur kenntniss der Kolbe'schen salicyl–sauresynthese. *J. Prakt. Chem.*, **31**, 397 (1885).

[9] O. Baine, G.F. Adamson, J.W. Barton, J.L. Fitch, D.R. Swayampati, H. Jeskey. The Kolbe–Schmitt reaction. II. The carbonation of phenols. *J. Org. Chem.*, **19**, 510 (1954).

[10] Ullmann's Encyclopedia of Industrial Chemistry, 5, Wiley-VCH, Weinheim, Germany (1997).

[11] J.C. Hessler. Some recent work in organic chemistry. *J. Am. Chem. Soc.*, **29**(1), 88 (1907).

[12] S. Tijmstra, C.A. Lobry de Bruyn. *Rec. Trav. Chim.*, **23**, 385 (1904).

[13] J.R. Johnson. Abnormal reactions of benzylmagnesium chloride. II. The mechanism of the *o*-tolyl rearrangement. *J. Am. Chem. Soc.*, **55**, 3029 (1933).

[14] A. Luttringhaus. *Annales*, **557**, 36 (1945).

[15] H. Gilman, C.E. Arntzen, F.J. Webb. Organometallic compounds in the Kolbe and Reimer–Tiemann reactions. *J. Org. Chem.*, **10**, 374 (1945).

[16] J.L. Hales, J.I. Jones, A.S. Lindsey. Mechanism of Kolbe–Schmitt reaction. *Chem. Ind.*, **49** (1954) Hales, J.L., Jones, J.I., Lindsey, A.S., (1954). Mechanism of the Kolbe–Schmitt reaction. I. Infrared studies. J. Am. Chem. Soc., Abstracts.

[17] D.C. Ayres. Carbanions in synthesis. pp. 168–173, Oldbourne Press, London (1966).

[18] M. Kunert, E. Dinjus, M. Nauck, J. Sieler. Structure and reactivity of sodium phenoxide. Following the course of the Kolbe–Schmitt reaction. *Chem. Ber./Recl.*, **130**(10), 1461 (1997).

[19] Y. Kosugi, Y. Imaoka, F. Gotoh, M.A. Rahim, Y. Matsui, K. Sakanishi. Carboxylations of alkali metal phenoxides with carbon dioxide. *Org. Biomol. Chem.*, **1**, 817 (2003).

[20] Z. Markovic, J.P. Engelbrecht, S. Markovic. Theoretical study of the Kolbe–Schmitt reaction mechanism. *Z. Naturforsch*, **57**(9–10), 812 (2002).

[21] M.J. Frisch, G.W. Trucks, H.B. Schlegel, G.E. Scuseria, M.A. Robb, J.R. Cheeseman, V.G. Zakrzewski, J.A. Montgomery Jr, R.E. Stratmann, J.C. Burant, S. Dapprich, J.M. Millam, A.D. Daniels, K.N. Kudin, M.C. Strain, O. Farkas, J. Tomasi, V. Barone, M. Cossi, R. B. Mennucci, C. Pomelli, C. Adamo, S. Clifford, J. Ochterski, G.A. Petersson, P.Y. Ayala, Q. Cui, K. Morokuma, A.D. Malick, K.D. Rabuck, K. Raghavachari, J.B. Foresman, J. Cioslowski, J.V. Ortiz, A.G. Baboul, B.B. Stefanov, G. Liu, A. Liashenko, P. Piskorz, I. Komaromi, R. Gomperts, R.L. Martin, D.J. Fox, T. Keith, M.A. Al-Laham, C.Y. Peng, A. Nanayakkara, M. Challacombe, P.M.W. Gill, B. Johnson, W. Chen, M.W. Wong, J.L. Andres, C. Gonzalez, M. Head-Gordon, E.S. Replogle, J.A. Pople Cammi. *Gaussian 98, Revision A.9*, Gaussian, Inc, Pittsburgh, PA (1998).

[22] I. Stanescu, L.E.K. Achenie (2005) A theoretical study of solvent effects on Kolbe–Schmitt reaction kinetics (submitted to Chemical Engineering Science).

[23] Jaguar 4.2, Schrodinger, LLC, Portland, OR (19912002).

[24] P.J. Hay, W.R. Wadt. *J. Chem. Phys.*, **82**, 270 Hay, P.J. and Wadt, W.R., (1985) J. Chem. Phys. 82, 284 (1985).

[25] J.C. Moseley, W. Edyvean, J. ("Shell" Refining & Marketing Co., Ltd.)British Patent 738,359 Hartley. Aromatic hydroxy carboxylic acids. (1955).

[26] R. Ueno, N. (Ueno Pharmaceutical Co.)US Patent 3,816,521 Tetsuya. Process for the production of *p*-hydroxybenzoic acid. (1974).

[27] A. Wacker. Manufacture of aromatic oxy-carboxylic acids. British Patent 384,619 (1932).

[28] Dow Chemical Co, Salicylic acid and its alkali metal salts. British Patent 949,988 (1964).

[29] G. Jansen, P. Wolff. Chemical process. (1983), US Patent 4,376,867

[30] L.B. (Monsanto Chemical Co.)US Patent 2,824,892 Barkley. Carboxylation of phenols. (1958).

[31] I. Hirao, K. Ota, S. Sueta, Y. Hara. Carboxylation of phenol derivatives. IV. Synthesis of *p*-hydroxybenzoic acid and salicylic acid from alkali phenoxides in *N*,*N*-dimethylformamide. *Yuki Gosei Kagaku Kyokaishi*, **25**(5), 412 (1967).

[32] M. Furuya, A. Nagatomo, M. (Mitsui Toatsu Chemicals, Inc., Japan)European Patent 834,494 A1 Wada. Preparation of hydroxybenzoic acids. (1998).

[33] S. Wideqvist. Some aspects of Kolbe's synthesis of salicylic acid. *Ark. Kemi*, **7**(26), 229 (1954).

[34] D.J. (Ilford Ltd.)British Patent 638,196 Fry. Hydroxy aromatic carboxylic acids. (1950).

[35] R. Gani, B. Nielsen, A. Fredenslund. A group contribution approach to computer-aided molecular design. *AIChE J.*, **37**(9), 1318 (1991).

[36] V. Venkatasubramanian, K. Chan, J.M. Caruthers. Computer-aided molecular design using genetic algorithms. *Comput. Chem. Eng.*, **18**(9), 833 (1994).

[37] L. Constantinou, K. Bagherpour, R. Gani, J.A. Klein, D.T. Wu. Computer aided product design: problem formulations, methodology and applications. *Comput. Chem. Eng.*, **20**, 685 (1996).

[38] A.P. Duvedi, L.E.K. Achenie. Designing environmentally safe refrigerants using mathematical programming. *Chem. Eng. Sci.*, **51**(15), 3727 (1996).

[39] N. Churi, L.E.K. Achenie. Novel mathematical programming model for computer aided molecular design. *Ind. Eng. Chem. Res.*, **35**(10), 3788 (1996).

[40] E.C. Marcoulaki, A.C. Kokossis. Molecular design synthesis using stochastic optimisation as a tool for scoping and screening. *Comput. Chem. Eng.*, **22**, S11 (1998).

[41] P.M. Harper, R. Gani. A multi-step and multi-level approach for computer aided molecular design. *Comput. Chem. Eng.*, **24**, 677 (2000).

[42] Y. Wang, L.E.K. Achenie. Computer aided solvent design for extractive fermentation. *Fluid Phase Equilib.*, **201**(1), 1 (2002).

[43] R. Gani. ICAS documentation. Computer Aided Process Engineering Center. Department of Chemical Engineering. Technical University of Denmark, Lyngby, Denmark (1999–2004).

[44] J. Barra, M.A. Pena, P. Bustamante. Proposition of group molar constants for sodium to calculate the partial solubility parameters of sodium salts using the van Krevelen group contribution method. *Eur. J. Pharm. Sci.*, **10**, 153 (2000).

[45] A.F.M. Barton. *CRC Handbook of Solubility Parameters and Other Cohesion Parameters*, 2, CRC Press, Boca Raton, FL (1991).

[46] D.J. Tannor, B. Marten, R.B. Murphy, R.A. Friesner, D. Sitkoff, A. Nicholls, M.N. Ringnalda, W.A. Goddard III, B. Honig. Accurate first principles calculation of molecular charge distributions and solvation energies from *ab initio* quantum mechanics and continuum dielectric theory. *J. Am. Chem. Soc.*, **116**, 11875 (1994).

[47] B. Marten, K. Kim, C. Cortis, R.A. Friesner, R.B. Murphy, M.N. Ringnalda, D. Sitkoff, B. Honig. New model for calculation of solvation free energies: correction of self-consistent reaction field continuum dielectric theory for short-range hydrogen-bonding effects. *J. Phys. Chem.*, **100**, 11775 (1996).